AMERICAN SOCIETY of
GENE & CELL
THERAPY

miR-217 Promotes Cardiac Hypertrophy and Dysfunction by Targeting PTEN

Xiang Nie,[1,2] Jiahui Fan,[1,2] Huaping Li,[1,2] Zhongwei Yin,[1,2] Yanru Zhao,[1,2] Beibei Dai,[1,2] Nianguo Dong,[3] Chen Chen,[1,2] and Dao Wen Wang[1,2]

[1]Division of Cardiology, Department of Internal Medicine, Tongji Hospital, Tongji Medical College, Huazhong University of Science and Technology, Wuhan 430030, China; [2]Hubei Key Laboratory of Genetics and Molecular Mechanisms of Ca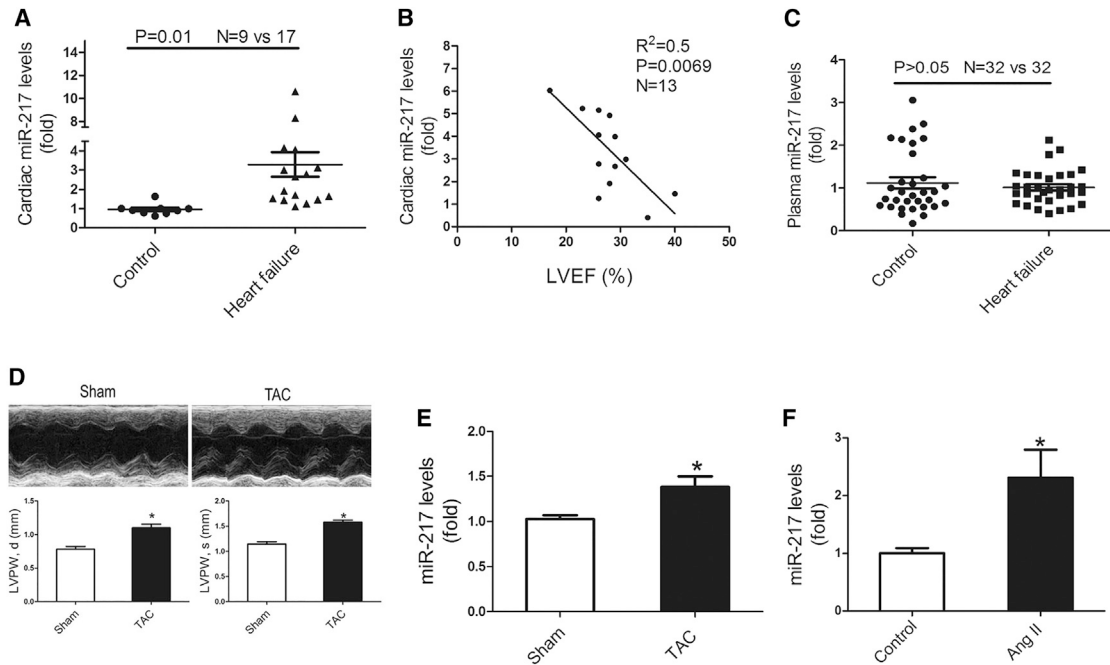rdiological Disorders, Huazhong University of Science and Technology, Wuhan 430030, China; [3]Department of Cardiovascular Surgery, Union Hospital, Tongji Medical College, Huazhong University of Science and Technology, Wuhan 430022, China

Previously, we found that the miR-217 expression level was increased in hearts from chronic heart failure (CHF) patients by using miRNA profile analysis. This study aimed to explore the role of miR-217 in cardiac dysfunction. Heart tissue samples from CHF patients were used to detect miR-217 expression levels. A type 9 recombinant adeno-associated virus (rAAV9) was employed to manipulate miR-217 expression in mice with thoracic aortic constriction (TAC)-induced cardiac dysfunction. Cardiac structure and function were measured by echocardiography and invasive pressure-volume analysis. The expression levels of miR-217 were increased in hearts from both CHF patients and TAC mice. Overexpression of miR-217 *in vivo* aggravated pressure overload-induced cardiac hypertrophy, fibrosis, and cardiac dysfunction, whereas miR-217-TUD-mediated downregulation of miR-217 reversed these effects. PTEN was predicted and validated as a direct target of miR-217, and re-expression of PTEN attenuated miR-217-mediated cardiac hypertrophy and cardiac dysfunction. Importantly, cardiomyocyte-derived miR-217-containing exosomes enhanced proliferation of fibroblasts *in vitro*. All of these findings show that miR-217 participates in cardiac hypertrophy and cardiac fibrosis processes through regulating PTEN, which suggests a promising therapeutic target for CHF.

INTRODUCTION

Cardiac hypertrophy is an adaptive response to hemodynamic stress to compensate for cardiac dysfunction with an increase in cardiomyocyte size, enhanced protein synthesis, and a higher organization of the sarcomere.[1,2] However, sustained stressful conditions, such as hypertension and valve diseases,[3,4] may lead to pathological cardiac hypertrophy, which is characterized by enlarged left ventricular diameter and cardiac dysfunction[1,5] and, ultimately, progress to heart failure, accounting for substantial morbidity and mortality worldwide.[6] The underlying mechanisms are not fully understood; fetal gene reactivation, energy metabolism abnormality, and enhanced protein synthesis may be involved in this progression.[2,7,8] Thus, in-depth studies are urgently needed.

MicroRNAs (miRNAs) are small non-coding RNAs 18–22 nt in length that induce gene silence by binding to the 3′ UTR of target

mRNAs.[9,10] Various miRNAs have been reported to play important roles in cardiac hypertrophy and heart failure. For example, miR-21-3p attenuates the cardiac hypertrophic response by targeting histone deacetylase-8,[11] whereas heart-specific overexpression of miR-206 in mice protects the heart from ischemia and reperfusion injury by targeting forkhead box protein P1.[12] Moreover, cardiac overexpression of miR-208a is sufficient to induce cardiac hypertrophy by repressing the expression of thyroid hormone-associated protein 1 and myosin.[13] miR-133 promotes cardiac hypertrophy through Rhoa and Cdc42 in thoracic aortic constriction (TAC)-induced mice.[14] These investigations indicate that miRNAs play significant roles in heart disease and may serve as promising therapeutic targets.

In previous studies, we identified dysregulated changes of several circulating miRNAs that could be ideal biomarkers for heart failure by comparing miRNAs expression patterns in both heart tissue and plasma samples from chronic heart failure (CHF) patients over controls. Global cardiac miRNA profile analysis revealed that miR-217, miR-216a-5p, miR-21-3p, miR-665, and miR-144-3p were the top five upregulated miRNAs in hearts from CHF patients.[15] However, in plasma, the level of miR-217 was unchanged. Consistently, increased expression of miR-217 was also found in hearts from thoracic aortic banding (TAB) mice or heart-specific transgenic mice expressing activated calcineurin A (CnATg), and the expression of miR-217 in the plasma was not measured.[16] Another study demonstrates that increased expression of miR-217 is detected in the hearts from TAB mice and in neonatal rat left ventricle myocytes treated with endothelin-1 (ET-1). Overexpression of miR-217 promotes pathological hypertrophy and fetal gene re-expression by targeting euchromatic histone lysine methyltransferase 1 (EHMT1/2).[17] These

Figure 1. Expression of miR-217 in Cardiac Hypertrophy and Dysfunction

(A) Real-time PCR analysis of miR-217 expression in human myocardial tissue (control, n = 9; heart failure [HF], n = 17) from chronic heart failure patients. (B) Linear correlation between miR-217 levels and LVEF %. (C) qPCR analysis of miR-217 expression in blood plasma (control, n = 32; HF, n = 32). (D) Hypertrophic parameters in sham and TAC mice; *p < 0.05 versus sham. (E) The levels of miR-217 in TAC-induced mouse hearts; n = 6, *p < 0.05 versus sham. (F) The expression of miR-217 in H9c2 cells treated with Ang II; n = 6, *p < 0.05 versus control. Data are shown as mean ± SEM.

findings indicate that miR-217 plays a significant role in cardiac dysfunction.

The heart is composed of diverse cellular components, including cardiomyocytes, fibroblasts, and endothelial cells. A number of studies have demonstrated the existence of a complex network among different cell types.[18] miRNAs have emerged as regulators of cell-cell communication and paracrine signaling mediators during heart disease.[19,20] Interestingly, miRNAs have been discovered in extracellular vesicles, which are small, membrane-derived particles. Exosomes are a well characterized subtype of secreted extracellular vesicles, which are endogenous nano-vesicles (30–100 nm) that can transfer biological messages and modulate signaling pathways in target cells.[21–23] A recent study showed that cardiac fibroblast-derived miR-21-3p-enriched exosomes promote cardiomyocyte hypertrophy through targeting sorbin, SH3 domain-containing protein 2 (SORBS2), and PDZ and LIM domain 5 (PDLIM5).[24] Cardiac progenitor cell-derived exosomal miR-21 inhibits apoptosis through downregulating PDCD4.[25]

Here we investigated the potential role of miR-217 in cardiac hypertrophy and heart failure, and the results showed that cardiac miR-217 expression was increased in TAC-induced mice. Moreover, overexpression of miR-217 promoted cardiac hypertrophy by targeting phosphatase and tension homolog deleted on chromosome ten

(PTEN) *in vivo* and *in vitro*. Furthermore, cardiomyocyte-derived exosomes promoted fibroblasts viability *in vitro*.

RESULTS

Expression of miR-217 in Cardiac Hypertrophy and Dysfunction

First, the expression levels of miR-217 in cardiac tissue and plasma from CHF patients and controls were measured. The results showed that the level of miR-217 was significantly increased in cardiac tissue compared with the control population (Figure 1A) and that the cardiac miR-217 expression level was negatively correlated with cardiac function, as indicated by the left ventricular ejection fraction percentage (LVEF %) (Figure 1B). However, the plasma miR-217 levels remained unchanged (Figure 1C). Moreover, echocardiographic analysis revealed that TAC induced cardiac hypertrophy in mice (Figure 1D). Consistently, increased expression of miR-217 was also detected in the hearts of TAC mice (Figure 1E). Finally, the expression of miR-217 was also increased in H9c2 cells treated with angiotensin II (Ang II) (Figure 1F). These results indicate that miR-217 may play a key role in cardiac hypertrophy and CHF.

miR-217 Promoted Cardiac Hypertrophy *In Vivo* and *In Vitro*

To investigate the role of miR-217 in cardiac hypertrophy, the type 9 recombinant adeno-associated virus (rAAV9) system was used in TAC-induced cardiac hypertrophic mice. As shown in Figure 2A, rAAV9 mainly induced miR-217 expression in the heart. We first
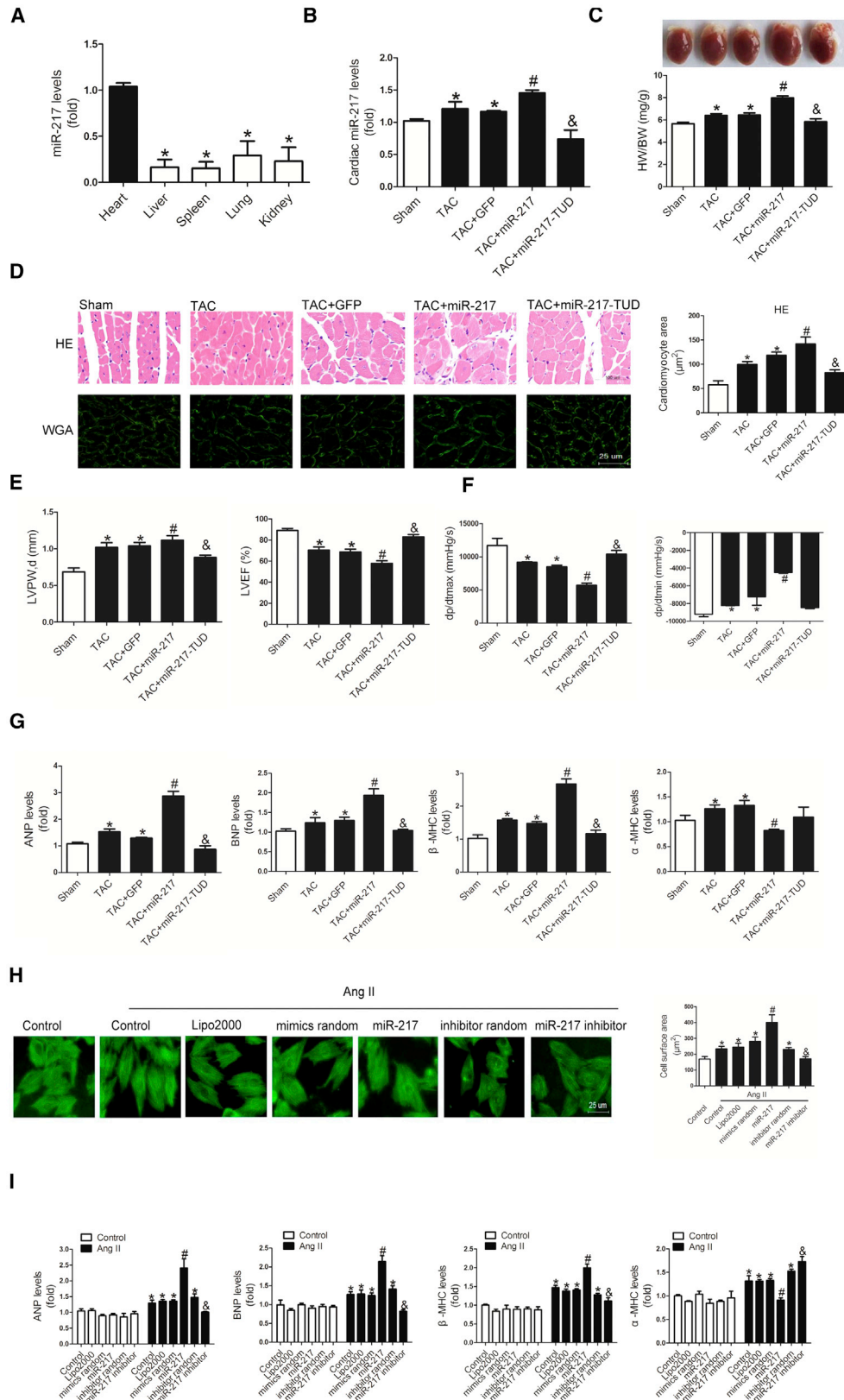
detected the effects of miR-217 on cardiac hypertrophy under normal conditions. We found that miR-217 slightly increased left ventricular posterior thickness but showed no effects on heart weight and cardiac function compared with control mice (Figure S1). Then we investigated the role of miR-217 under stress conditions. Overexpression of miR-217 aggravated cardiac hypertrophy, as indicated by increased heart size and heart weight/body weight radio in TAC mice, whereas rAAV9-miR-217-TUD reversed these effects (Figures 2B and 2C). Furthermore, the cardiomyocytes cross-sectional area determined by staining with H&E or wheat germ agglutinin (WGA) were increased in rAAV9-miR-217 mice (Figure 2D). These results indicated that miR-217 overexpression promoted cardiac hypertrophy induced by TAC, whereas miR-217 inhibition prevented cardiac hypertrophy.

Cardiac structure and function were evaluated by echocardiography and invasive pressure-volume analysis, respectively. Echocardiographic analysis showed a marked increase in diastolic left ventricular posterior thickness but a decrease in LVEF % in TAC mice compared with control mice (Table S4; Figure 2E). Consistently, overexpression of miR-217 aggravated cardiac dysfunction in mice induced by TAC, whereas miR-217-TUD alleviated cardiac dysfunction detected by Millar cardiac catheter (Table S5; Figure 2F). These results were further supported by changes in the expression levels of heart failure biomarkers ANP, BNP, β-major histocompatibility complex (MHC), and α-MHC (Figure 2G). *In vitro* experiments were also carried out. H9c2 cells were transfected with miR-217 and miR-217 inhibitor and then treated with Ang II. Similarly, miR-217 promoted Ang II-induced cell hypertrophy indicated by fluorescein isothiocyanate (FITC)-phalloidin staining, whereas the miR-217 inhibitor attenuated this effect (Figure 2H). Consistent with the *in vivo* data above, miR-217 enhanced the expression of ANP, BNP, and β-MHC but downregulated the expression of α-MHC, whereas the miR-217 inhibitor had the opposite effect (Figure 2I). These results were further confirmed in experiments performed with primary cardiac myocytes (Figure S2). All of these results indicated that miR-217 promoted cardiac hypertrophy and dysfunction.

miR-217 Binds to the 3′ UTR of PTEN

Target genes of miR-217 were predicted in Targetscan, which yielded 200 candidate genes. After pathway and gene ontology (GO) analysis, we obtained 25 potential target genes that may be involved in heart diseases. However, only five of them are conserved among humans, mice, and rats in the 3′ UTR: PTEN, PDE5A, ATG7, MAPK1, and ANLN. Then, RNA co-immunoprecipitation with anti-Ago2 antibodies was performed to detect the putative targets of miR-217. The results showed that miR-217 transfection significantly increased the binding mRNA levels of PTEN and PDE5A (Figure 3A). Because PTEN was the highest increased mRNA and the cardiac expression of PTEN was decreased in TAC mice compared with control mice, PTEN was chosen as the potential target of miR-217 (Figure 3B). Next, the 3′ UTR of PTEN was constructed to luciferase reporter plasmid for co-transfection to HEK293T cells with random mimics or miR-217. The results showed that the relative luciferase activity of the PTEN 3′ UTR reporter treated with miR-217 was significantly suppressed compared with transfection with random mimics or the mutant reporter or empty vector transfected with miR-217 (Figure 3C). Furthermore, the level of PTEN in H9c2 cells transfected with miR-217 was suppressed compared with random mimics detected by western blots (Figure 3D).

Restored PTEN Eliminated the Effects of miR-217 Overexpression in Cardiac Hypertrophy

To further explore the role of the miR-217/PTEN pathway in cardiac hypertrophy, we restored the expression of PTEN in miR-217-treated TAC mice using rAAV9-PTEN. Real-time PCR assays showed that miR-217 suppressed the mRNA expression of PTEN in TAC-induced mice, whereas rAAV9-PTEN restored PTEN expression (Figure 4A). Similar results were also found by western blots (Figure 4B). PTEN reexpression alleviated the hypertrophic effects of miR-217 overexpression in TAC-induced mice, as indicated by decreased heart size and heart weight/body weight ratio, compared with miR-217-treated TAC mice (Figure 4C). The results were also confirmed by cardiomyocyte cross-sectional area, determined by HE staining and WGA staining (Figure 4D). Echocardiography and invasive pressure-volume measurements showed that restored PTEN expression reversed not only cardiac dysfunction in rAAV9-miR-217-treated TAC mice (Tables S6 and S7; Figures 4E and 4F) but also the slightly increased wall thickness in rAAV9-miR-217-treated normal mice (Tables S8 and S9). In addition, restored PTEN expression reversed the effects of miR-217 in the expression of heart failure markers, including ANP, BNP, β-MHC, and α-MHC (Figure 4G).

Figure 2. miR-217 Promoted Cardiac Hypertrophy *In Vivo* and *In Vitro*

(A) rAAV9 mediated miR-217 expression in the heart, liver, spleen, lungs, and kidneys. *p < 0.05 versus sham. (B) Cardiac expression of miR-217 was detected by real-time PCR assays; *p < 0.05 versus sham, #p < 0.05 versus TAC+GFP, &p < 0.05 versus TAC+GFP. (C) The ratio of heart weight to body weight (HW/BW) and heart size of mice; *p < 0.05 versus sham, #p < 0.05 versus TAC+GFP; &p < 0.05 versus TAC+GFP. (D) H&E and WGA staining of transverse sections of cardiomyocytes from TAC-induced mice with various treatments. Scale bars, 100 μm and 25 μm. The size of cardiomyocytes was quantified by measuring the transverse cell area. *p < 0.05 versus sham, #p < 0.05 versus TAC+GFP; &p < 0.05 versus TAC+GFP. (E) Echocardiography analysis of cardiac function in TAC-induced mice. LVPW,d, left ventricle posterior wall thickness at diastole; EF, ejection fraction. *p < 0.05 versus sham; #p < 0.05 versus TAC+GFP, &p < 0.05 versus TAC+GFP. (F) Hemodynamic parameters measured with the Millar cardiac catheter system in mice with different treatments. dp/dt$_{max}$, peak instantaneous rate of left ventricular pressure increase; dp/dt$_{min}$, peak instantaneous rate of left ventricular pressure decline. *p < 0.05 versus sham, #p < 0.05 versus TAC+GFP, &p < 0.05 versus TAC+GFP. (G) Relative expression of cardiac hypertrophy marker genes of heart samples from variously treated mice detected by real-time PCR; *p < 0.05 versus sham, #p < 0.05 versus TAC+GFP, &p < 0.05 versus TAC+GFP. (H) Measurement of the surface area of H9c2 cells by FITC-phalloidin staining. Scale bar, 25 μm. *p < 0.05 versus control, #p < 0.05 versus Ang II+random mimics, &p < 0.05 versus Ang II+inhibitor random. (I) The expression of markers of cardiac hypertrophy were detected by real-time PCR in H9c2 cells with various treatments; *p < 0.05 versus control, #p < 0.05 versus Ang II+mimics random, &p < 0.05 versus Ang II+inhibitor random. Data are shown as mean ± SEM.
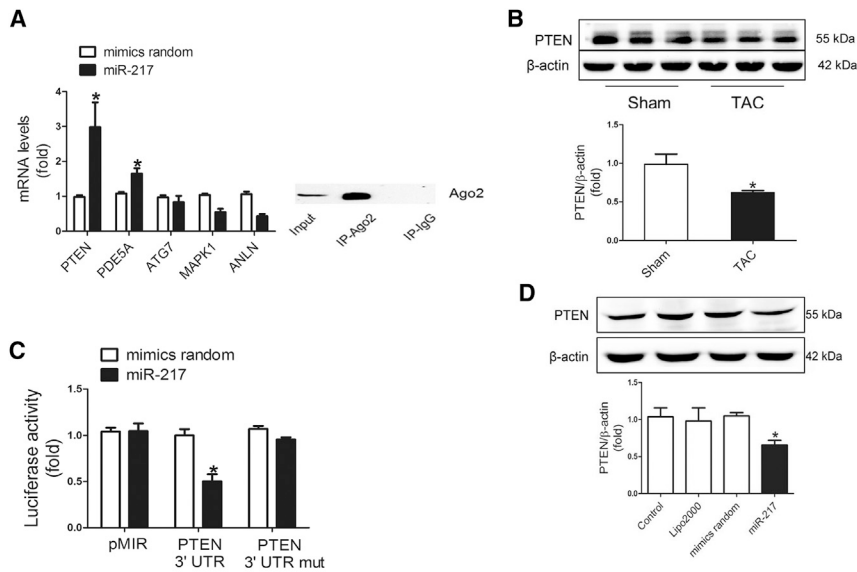
Figure 3. miR-217 Binds to the 3′ UTR of PTEN

(A) The levels of mRNA in miR-217-transfected cells detected by RNA binding protein immunoprecipitation; *p < 0.05 versus random mimics. (B) The expression of PTEN in TAC mice; *p < 0.05 versus sham. (C) Luciferase activity was determined; n = 3, *p < 0.05 versus random mimics. (D) The protein level of PTEN was examined by western blot analysis from variously treated H9c2 cells; *p < 0.05 versus random mimics.

Further, the roles of PTEN in cardiac hypertrophy were investigated *in vitro*. Small interfering RNA (siRNA)-PTEN (si-PTEN) was used to downregulate PTEN expression in H9c2 cells. Three si-PTENs were designed, and the third one (si-PTEN-3) most efficiently inhibited its expression (Figure 5A). As shown in Figure 5B, si-PTEN aggravated Ang II-induced cell hypertrophy, as found by measuring the cell surface area. Real-time PCR assays showed that si-PTEN upregulated the expressions of ANP, BNP, and β-MHC but decreased α-MHC expression (Figure 5C). These findings were further confirmed in primary cardiac myocytes (Figure S3).

PTEN plays a significant role in cardiac hypertrophy by dephosphorylating phosphatidylinositol 3,4,5-trisphosphate (PIP3) to inactive the AKT pathway, which is important for cell growth in cardiac hypertrophy.[26] We found that p-AKT/AKT levels were elevated in miR-217-treated mice, whereas restored PTEN expression attenuated the effects of miR-217 (Figure 5D). All of these results indicate that miR-217 aggravates cardiac hypertrophy and dysfunction by suppressing PTEN expression to active the AKT pathway.

Cardiomyocyte-Derived miR-217-Enriched Exosomes Promoted Fibroblast Viability

Further, we found that miR-217 aggravated TAC-induced myocardial fibrosis, as detected by Masson and Sirius Red staining (Figure 6A). Thus, the expression of miR-217 in cultured human cardiomyocytes and human fibroblasts was measured to determine the cell type distribution. Treatment with Ang II increased the expression of miR-217 in human cardiomyocytes rather than in human fibroblasts (Figure 6B). The expression of miR-217 in primary cardiomyocytes and fibroblasts from hearts of control and TAC mice were measured, respectively. As shown in Figure 6C, miR-217 was enriched in cardiomyocytes compared with fibroblasts in sham mice, but it was increased in both cell types in TAC-induced mice. Thus, we tried to investigate the

potential paracrine miRNA crosstalk between cardiomyocytes and cardiac fibroblasts. Exosomes were purified from cellular supernatant treated with Ang II or miR-217 detected by CD63 protein expression and electron microscope (Figures 6D and 6E). The expression level of miR-217 was increased in exosomes from H9c2 cells treated with Ang II or miR-217 (Figure 6F). CD63 levels were also increased in miR-217-treated mice, as detected by immunohistochemistry (Figure 6G). Importantly, miR-217-containing exosomes promoted fibroblasts viability, as detected by cell count kit-8 assays (Figure 6H). Marker genes expression of fibrosis, such as colα1, colα2, and fibronectin, was also increased in exosome-treated fibroblasts (Figure 6I).

DISCUSSION

Previously, we reported that miR-217 was highly expressed in the hearts of CHF patients by using miRNA arrays.[15] The current study showed that cardiac miR-217 was upregulated in pressure overload-induced hypertrophic mice. rAAV9-mediated expression of miR-217 in TAC-induced mice demonstrates that overexpression of miR-217 aggravates TAC-induced cardiac hypertrophy and dysfunction. Conversely, rAAV9-miR-217-TUD mice protected the heart from pathological hypertrophy induced by pressure overload.

MiR-217 lies in human chromosome 2 and mouse chromosome 11, which is conserved among humans, rats, and mice.[27] Recently, many studies have shown that miR-217 plays multiple roles in physiological and pathological processes. For example, mir-217 promotes inflammation and fibrosis in high-glucose-cultured rat glomerular mesangial cells via the Sirt1/HIF-1α signaling pathway.[28] MiR-217 mediates the protective effects of the dopamine D2 receptor on fibrosis by targeting Wnt5a in human renal proximal tubule cells.[29] Overexpression of transforming growth factor β1 (TGF-β1) triggers deregulation of the miR-217-SIRT1 pathway and then promotes the epithelial-mesenchymal transition process.[30]
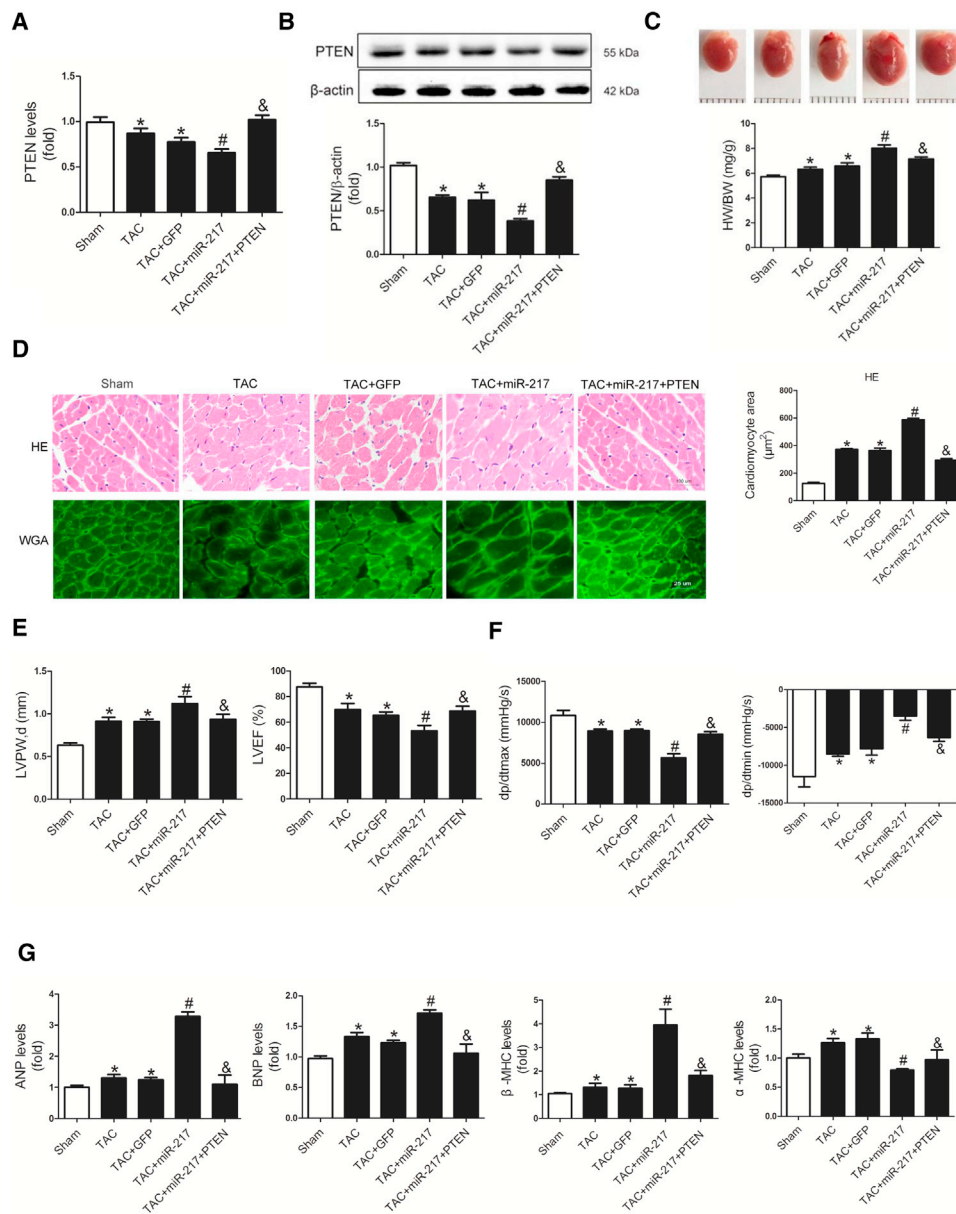
In this study, we used the rAAV9 gene delivery system to induce miR-217 expression in the heart. Previous studies showed that rAAV9 has a preference for heart tissue in terms of transduction efficiency and transgene expression compared with rAAV2 and rAAV8.[31] However, rAAV9-delivered miR-217 may also target

Figure 4. Restored PTEN Eliminated the Effects of miR-217 Overexpression in Cardiac Hypertrophy

(A) Cardiac expression of PTEN was detected by real-time PCR assays; *p < 0.05 versus sham, #p < 0.05 versus TAC+GFP, &p < 0.05 versus TAC+miR-217. (B) The protein level of PTEN was measured by western blot; *p < 0.05 versus sham, #p < 0.05 versus TAC+GFP, &p < 0.05 versus TAC+miR-217. (C) The ratio of HW/BW and heart size of mice; *p < 0.05 versus sham, #p < 0.05 versus TAC+GFP, &p < 0.05 versus TAC+miR-217. (D) H&E staining and WGA staining of transverse sections of cardiomyocytes from TAC-induced mice with various treatments. Scale bars, 100 μm and 25 μm. The size of cardiomyocytes was quantified by measuring the transverse cell area; *p < 0.05 versus sham, #p < 0.05 versus TAC+GFP, &p < 0.05 versus TAC+miR-217. (E) Echocardiography analysis of cardiac function in TAC-induced mice; *p < 0.05 versus sham, #p < 0.05 versus TAC+GFP, &p < 0.05 versus TAC+miR-217. (F) Hemodynamic parameters were measured with the Millar cardiac catheter system in mice with different treatments; *p < 0.05 versus sham, #p < 0.05 versus TAC+GFP, &p < 0.05 versus TAC+miR-217. (G) The expression of cardiac hypertrophy marker genes of heart samples from variously treated mice was detected by real-time PCR; *p < 0.05 versus sham, #p < 0.05 versus TAC+GFP, &p < 0.05 versus TAC+miR-217. Data are shown as mean ± SEM.

other organs, such as the liver and kidney, and may also exert functions on these organs; thus, potential systemic effects of miR-217 should not be ruled out.[32] Organ-specific miR-217 transgenic or knockout mice can be used to regulate miR-217 expression in the heart to further explore the role of miR-217 in cardiac hypertrophy and heart failure.
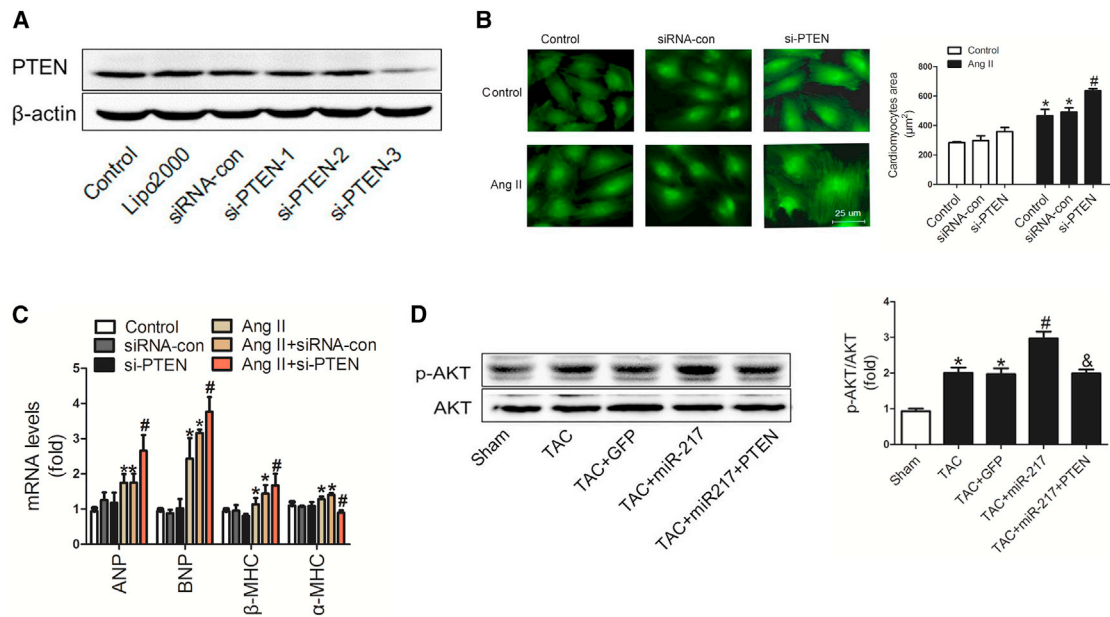
Figure 5. si-PTEN Aggravated Cardiac Hypertrophy *In Vitro*

(A) The efficiency of siRNA on PTEN expression was detected by western blot. (B) Measurement of the surface area of H9c2 cells transfected with siRNA control (siRNA-con) or si-PTEN. Scale bar, 25 mm. Also shown is quantification of the size of H9c2 cells; n = 3, *p < 0.05 versus control, #p < 0.05 versus Ang II+siRNA-con. (C) The expression of marker genes of cardiac hypertrophy in si-PTEN-treated H9c2 cells was detected by real-time PCR; n = 3, *p < 0.05 versus control; #p < 0.05 versus Ang II+siRNA-con. (D) The protein levels of p-AKT/AKT in TAC-induced mice; *p < 0.05 versus sham, #p < 0.05 versus TAC+GFP, &p < 0.05 versus TAC+miR-217. Data are shown as mean ± SEM.

Using bioinformatics and RNA co-immunoprecipitation analysis, we predicted and validated PTEN as a direct target of miR-217. PTEN is a membrane-bound lipid phosphatase and functions essentially as a negative regulator of the phosphatidylinositol 3-kinase (PI3K)/AKT pathway.[33,34] PTEN is universally expressed in cardiomyocytes, fibroblasts, and endothelial cells and plays important roles in cell survival, hypertrophy, contractility, and metabolism.[35] Cardiomyocyte-specific inactivation of PTEN results in cardiac hypertrophy and a dramatic decrease in cardiac contractility via the PI3K/AKT signaling pathway. PI3Kα mediates alteration in cell size, whereas PI3Kβ acts as a negative regulator of cardiac contractility.[26] Other studies also showed that the tyrosine kinase-receptor p110-PTEN pathway is a critical regulator of cardiac cell size,[36] and the G protein-coupled receptor (GPCR)-linked PI3Kβ-PTEN signaling pathway modulates heart muscle contractility.[37] Recently, it was found that miR-22 promotes Ang II-induced rat cardiomyocyte hypertrophy by targeting PTEN.[38] All of this indicates that PTEN plays a significant role in heart disease, especially in cardiac hypertrophy. In the current study, we constructed rAAV9-PTEN to restore PTEN expression in rAAV9-miR-217 TAC-induced mice, and the results showed that restoring PTEN attenuated miR-217-induced cardiac hypertrophy and dysfunction. On the other hand, si-PTEN promoted Ang II-induced cell hypertrophy *in vitro*, which is consistent with the effects of miR-217 on cardiac hypertrophy. These results suggest that PTEN is a direct target of miR-217 and that the miR-217/PTEN pathway plays a significant role in cardiac hypertrophy. However, one single miRNA

can regulates dozens to hundreds of targets simultaneously. Genome-wide measurements of the effects of miRNAs on protein and mRNA levels have demonstrated that the degradation of miRNA targets is a about 66%–90% and that translational repression accounts for 6%–26% of the miRNA-mediated repression observed in cultured mammalian cells.[39] However, the exact repression efficiency of one miRNA on one specific target gene has not been fully elucidated. One study indicated that miR-320 regulated cardiac ischemia and re-perfusion injury by targeting Hsp20, which accounts for almost 30% of repression of Hsp20.[40] Another study showed that miR-25 reduced 40% of the levels of the target gene IP3R1 in the failing heart and that miRNA-208a promoted cardiac hypertrophy by targeting Thrap1 and myostatin, whose inhibition efficiency is about 20% to 50% in mice.[41] The downstream signaling network may exhibit interaction effects or a cascade reaction, which means that a mild trigger may lead to a tremendous end. In our study, PTEN is one of the targets of miR-217 on which the repression effect of miR-217 is about 40%, which is the average inhibition efficiency of miRNAs. MiR-217 may also target other genes, such as EHMT1, in cardiac hypertrophy, as reported by other researchers.[17] Therefore, we think that PTEN is one of the main targets of miR-217 in cardiac hypertrophy, but we cannot exclude possible roles of other potential targets of miR-217 that may also contribute to cardiac hypertrophy.

Cardiac remodeling is a common response to chronic and acute cardiac injury, characterized by interstitial fibrosis and cardiac
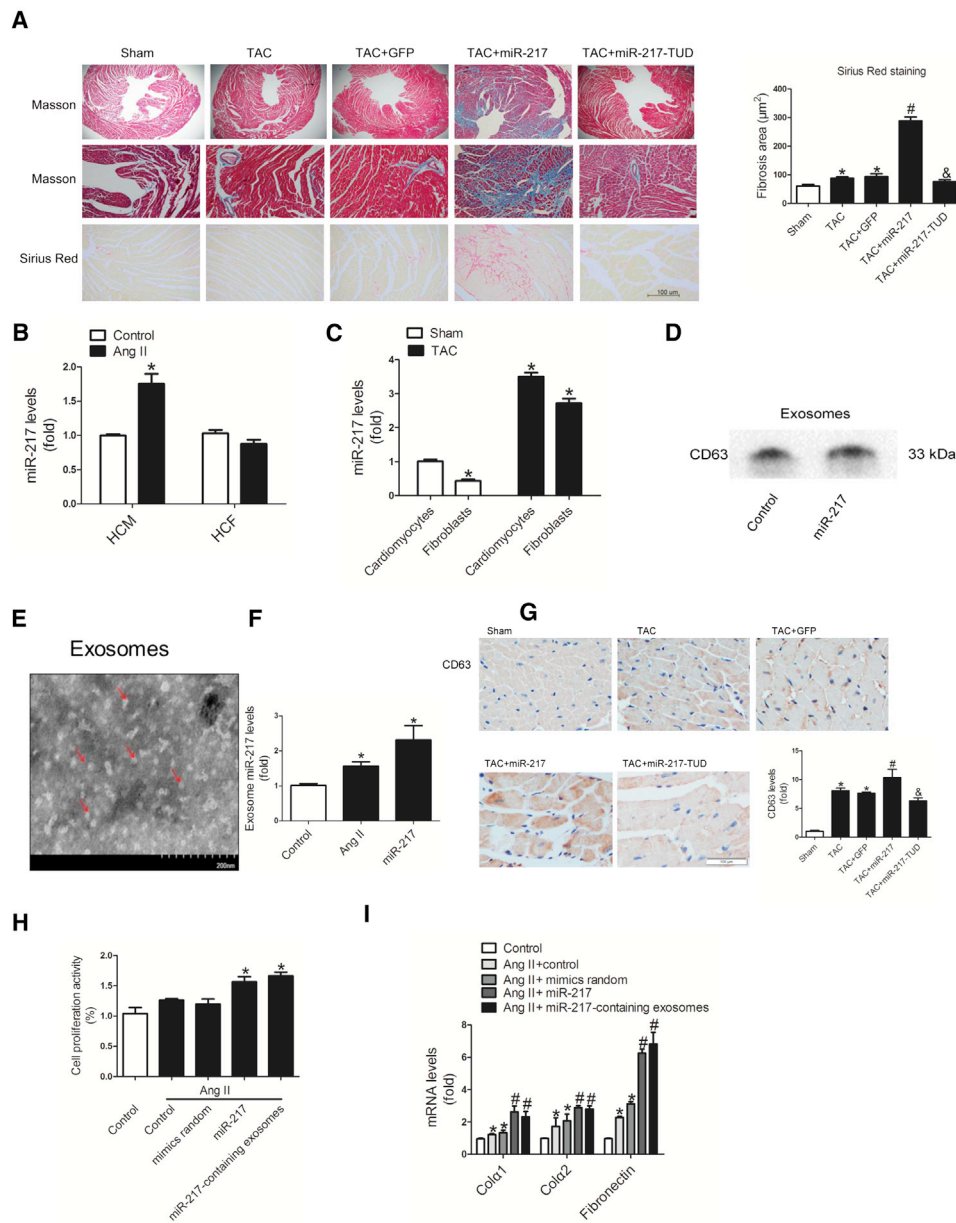
Figure 6. Cardiomyocyte-Derived miR-217-Enriched Exosomes Promoted Fibroblast Viability

(A) miR-217 promoted cardiac fibrosis, as detected by Masson and Sirius Red staining in TAC-induced mice; *$p < 0.05$ versus sham; #$p < 0.05$ versus TAC+GFP, &$p < 0.05$ versus TAC+GFP. (B) The expression of miR-217 in human cardiomyocytes and human cardiac fibroblasts treated with Ang II; *$p < 0.05$ versus control. (C) The distribution of miR-217 in primary cardiomyocytes and primary cardiac fibroblasts; *$p < 0.05$ versus sham. (D) Exosomes detected by western blot for CD63. (E) Exosomes detected by electron microscopy. (F) The expression of miR-217 was increased in exosomes, as measured by real-time PCR; *$p < 0.05$ versus control. (G) The level of CD63 in miR-217-treated mice was increased, as detected by immunohistochemical staining; *$p < 0.05$ versus sham; #$p < 0.05$ versus TAC+GFP; &$p < 0.05$ versus TAC+GFP. (H) miR-217-containing exosomes promoted fibroblast viability, as detected by cell count-8 assays; *$p < 0.05$ versus control. (I) The expression of colα1, colα2, and fibronectin in miR-217-containing, exosome-treated fibroblasts; *$p < 0.05$ versus control; #$p < 0.05$ versus Ang II + random mimics.

hypertrophy.[42] Under disease conditions, such as hypertension and valve disease, myocytes undergo diverse functional, structural, and metabolic abnormalities, such as sarcomere disorganization and hypertrophy, as well as activation of fibroblasts and interstitial and peri-vascular fibrosis, which ultimately lead to left ventricular hypertrophy, dilatation, and heart failure.[43] Recent studies have shown that the interactions between cardiac fibroblasts and cardiomyocytes are essential for progression of cardiac remodeling. Many factors
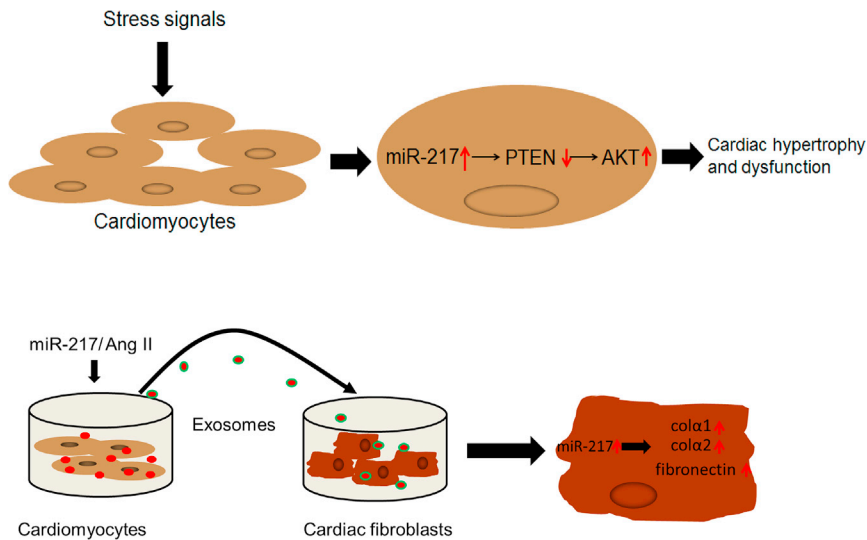
Figure 7. The Function of miR-217 in Cardiac Hypertrophy

Stress conditions induced cardiac miR-217 expression, and overexpression of miR-217 aggravated TAC-induced cardiac hypertrophy and dysfunction by targeting PTEN to activate the AKT pathway. *In vitro*, cardiomyocyte-derived miR-217-containing exosomes promoted fibroblasts viability and increased the expression of colα1, colα2, and fibronectin.

that exosomes mediate a number of paracrine signals; for example, vesicles secreted by the shear-responsive transcription factor Krüppel-like factor 2 (KLF2)-transduced or shear-stress-stimulated human umbilical vein endothelial cells (HUVECs) are enriched in miR-143/145 and regulate target gene expression in co-cultured smooth muscle cells (SMCs).[50] Other studies showed that exosomes are present in body fluids; for example, cardiac pressure overload-induced AT1R-enriched exosomes target cardiomyocytes, skeletal myocytes, and mesenteric resistance vessels to confer blood pressure response to Ang II infusion in AT1R knockout mice.[51] Human pericardial fluid contains exosomes enriched with cardiovascularly expressed miRNAs (e.g., let-7b-5p, miR-21-5p, and miR-23a-5p) are more abundant than plasma and promote therapeutic angiogenesis.[52] Selective packaging of miRNAs into vesicles may be crucial for the specificity of the biological functions of secreted miRNAs, and the mechanisms need to be studied further.

participate in this progression, especially non-coding RNAs. Overexpression of nicotinamide adenine dinucleotide phosphate (NADPH) oxidase 4 mediates Ang II-induced cardiac hypertrophy and cardiac fibrosis by activating the AKT/mTOR/nuclear factor κB (NF-κB) pathway.[44] *In vivo* inhibition of miR-133 by a single infusion of antagomir caused marked and sustained cardiac hypertrophy,[14] whereas cardiac overexpression of miR-133a prevented cardiac fibrosis via the ERK1/2 and SMAD-2 pathway.[45] Moreover, miR-133a overexpression decreased hypertrophy-associated myocardial fibrosis and cardiomyocyte apoptosis.[46] Exosome-mediated transfer of mRNA and miRNAs is a novel mechanism of genetic exchange between cells. It was found that Ang II stimulates release of exosomes from cardiac fibroblasts to upregulate rennin angiotensin system (RAS) in cardiomyocytes via activation of mitogen-activated protein kinases (MAPKs) and AKT, which promotes cardiac hypertrophy.[47] Macrophage-derived miR-155-containing exosomes inhibit cardiac fibroblast proliferation by downregulating son of sevenless homolog 1 (SOS1) expression and promotes inflammation by decreasing suppressor of cytokine signaling 1 (SOCS1) expression.[48]

Our study showed that the expression of miR-217 was significantly increased in the failing heart but remained unchanged in the plasma in CHF patients. Thus, we focused on the delivery and distribution of cardiomyocyte-derived miR-217, and we found a novel miRNA- and/or exosome-mediated communication between cardiomyocytes and cardiac fibroblasts. This indicates that miR-217 may play a role as a paracrine factor, not an endocrine one. In the *in vitro* study, we found that the expression of miR-217 was increased in exosomes from cardiomyocytes, indicating that miR-217 can be exported from cardiomyocytes via exosomes and transported to neighboring cells. However, the secretory mechanism and biological function of extracellular miRNAs remain unclear. Another study has shown that miR-217 can be a potential biomarkers of acute exocrine pancreatic toxicity in rats.[49] Different disease models with different damaged organs may lead to different organ distributions. Some studies showed

In summary, our findings reveal that miR-217 is highly expressed in the hearts of CHF patients and aggravate pressure overload-induced cardiac hypertrophy and dysfunction by suppressing PTEN expression. Cardiomyocyte-derived miR-217-containing exosomes induce fibroblast proliferation and may promote cardiac fibrosis (Figure 7). These findings suggest that miR-217 plays important roles in cardiac hypertrophy and dysfunction, providing therapeutic targets for heart failure.

MATERIALS AND METHODS
Materials
DMEM and fetal bovine serum (FBS) were obtained from Transgen Biotech (Beijing, China). Exosome-free FBS was from SBI (San Francisco, CA). Ang II, FITC-phalloidin, and FITC-WGA were from Sigma-Aldrich (St. Louis, MO). Antibodies against BNP and ANP were purchased from Abcam (Cambridge, MA), whereas PTEN, p-AKT, total AKT, β-actin, and CD63 were from Proteintech (Chicago, IL). Plasmid purification kits were from TIANGEN (Beijing, China). Chemically synthesized miRNAs, siRNAs, and exosome isolation reagent were obtained from RiboBio (Guangzhou, China).

Human Samples
This study was approved by the Ethics Review Board of Tongji Hospital and Tongji Medical College and conformed to the principles of the

Declaration of Helsinki. Informed consent was obtained from patients. Seventeen heart samples were collected from cardiac transplant patients with CHF, and nine heart samples were from accident victims. The baseline characteristics of the patients are listed in Table S1. Plasma samples from 32 normal controls and 32 CHF patients were enrolled in a second cohort, and the baseline data are listed in Table S2.

RNA Extraction and Real-Time PCR
Total RNA was extracted using Trizol (Invitrogen, Carlsbad, CA) and transcribed to cDNA using the Moloney murine leukemia virus (M-MLV) First-Strand cDNA Synthesis Kit according to the manufacturer's instructions (Invitrogen, Carlsbad, CA). The expression of miR-217 and mRNA was quantified by real-time qPCR using Power SYBR Green PCR Master Mix (Invitrogen, Carlsbad, CA) on a 7900HT FAST real-time PCR system (Life Technologies, Carlsbad, CA). The primers for mRNA detection are listed in Table S3. The results were analyzed using the $2^{-\Delta\Delta Ct}$ method as described previously.[53] Each experiment was repeated three times independently.

rAAV
rAAV9 vectors containing hsa-miR-217, hsa-miR-217-TUD, PTEN, or GFP were constructed by triple plasmid co-transfection, respectively, as described previously.[32] The vectors were purified and stored at −80°C before injection.

Animals
The study was approved by the Institutional Animal Research Committee of Tongji Medical College. All animal experimental protocols complied with the Guide for the Care and Use of Laboratory Animals published by the NIH and Animal Research: Reporting of In Vivo Experiments (ARRIVE). Male C57BL/6 mice (10 weeks old) were purchased from the Experimental Animal Center of Hubei (Wuhan, China). Mice were randomly divided into groups (n = 20/group) as follows: sham, TAC, TAC+rAAV9-GFP, TAC+rAAV9-miR-217, TAC+rAAV9-miR-217-TUD, and TAC+rAAV9-miR-217+PTEN. rAAV9 vectors (1 × 10^{11} virion particles in 100 μL saline solution) were administrated via the tail vein. Two weeks after the rAAV9 injection, pressure overload was induced by TAC. A 7-0 polypropylene suture was looped around the aortic arch, and a stenosis was placed using a 27G needle as a space holder. The sham mice underwent the same operation without aortic constriction. Two weeks after the operation, all animals were anesthetized with intraperitoneal injections of a xylazine (5 mg/kg) and ketamine (80 mg/kg) mixture and sacrificed, and organs were collected and frozen in liquid nitrogen, followed by storage at −80°C.

Echocardiography and Hemodynamic Detection
Echocardiography analysis was performed using a high-resolution imaging system with a 30-MHz high-frequency scanhead (VisualSonics Vevo770, VisualSonics, Toronto, Canada) as described previously.[54] The pressure-volume catheter (Millar 1.4F, SPR835, Millar Instruments, Houston, TX) was inserted into the left ventricle to measure instantaneous intraventricular pressure and volume as described previously.[11]

Cell Culture
H9c2 cells and 3T3 cells were obtained from the ATCC (Manassas, VA). The cells were cultured in DMEM supplemented with 10% FBS in a humidified atmosphere of 95% air and 5% CO_2 at 37°C. Human cardiomyocytes and human cardiac fibroblasts were purchased from ScienCell Research Laboratories (San Diego, CA) and cultured as indicated by the manufacturer.

Cells were transfected with random mimics, miR-217, miR-217 inhibitor, or siRNA targeting rat PTEN using Lipofectamine 2000 (Invitrogen, CA) separately following the manufacturer's protocol. Twenty-four hours after transfection, cells were treated with 1 mM Ang II and then collected 24 hr later. Each experiment was repeated at least three times independently.

Isolation of Cardiomyocytes
Newborn (1-day-old) rat hearts were isolated and placed in ice-cold Hanks' medium and cut into pieces. Then the tissues were digested with trypsin and type II collagenase at 37°C. The cells were passed through a cell strainer (200 mesh), centrifuged at 1,000 g for 10 min, and then seeded onto Petri dishes and incubated for 2 hr at 37°C. The supernatant (cardiomyocytes) was plated in DMEM. Primary cells were identified by immunofluorescence staining with the cardiomyocyte-specific marker a2-actin (ACTN2, Sigma), the fibroblast-specific antigen prolyl-4-hydroxylase (P4HB, Acris), and the endothelial cell marker CD31 (PECAM1, Abcam) as described previously.[11]

Western Blot
Protein from cells or frozen animal tissues with various treatments were extracted and homogenized in ice-cold lysis buffer. Lysates (20 mg protein/lane) were subjected to 10% SDS-PAGE gel for separation and transferred onto polyvinylidene fluoride (PVDF) membranes. After blocking non-specific sites with 5% BSA for 2 hr at room temperature, the membranes were incubated with primary antibodies overnight at 4°C. After washing with Tris-buffered saline Tween (T-BST), the membranes were incubated with a peroxidase-conjugated secondary antibody for 2 hr at room temperature. The bands were visualized with enhanced chemiluminescence reagents according to the manufacturer's recommendations. Each experiment was repeated at least three times independently.

Histological Analysis
Heart samples were fixed with 4% paraformaldehyde, embedded in paraffin, and finally sectioned into 4-mm slices. The morphology was detected by H&E staining, WGA, Masson, and Sirius Red staining and measured by Image-Pro Plus Version 6.0 software (Media Cybermetics, Washington).

FITC-Phalloidin Staining
Cells were washed with PBS and fixed in 4% paraformaldehyde for 10 min followed by incubation in 0.1% Triton X-100 for 10 min. After washing with PBS, cells were incubated in FITC-phalloidin at 4°C

overnight, and cells were subsequently visualized under a Nikon DXM1200 fluorescence microscope and measured by Image-Pro Plus Version 6.0 software (Media Cybermetics, Washington).

RNA Immunoprecipitation

Lysed cell extracts were immunoprecipitated with anti-Ago2 antibody (Abnova, Taiwan, China) or immunoglobulin G (IgG) (Santa Cruz Biotechnology, Santa Cruz, CA) using protein G Sepharose beads. After elution from the beads, bound RNA was extracted with Trizol and quantified by real-time PCR as described previously.[32]

Luciferase Assay

The wild-type or mutant 3′ UTR of the human PTEN gene was cloned into the pMIR-REPORT luciferase vector (Ambion, Carlsbad, CA). For luciferase reporter assays, miR-217 or random mimics was co-transfected with the pMIR-PTEN 3′ UTR or the empty vector, respectively, as well as the pRL-TK plasmid (Promega, Madison, WI) using Lipofectamine 2000 in 293T cells. Luciferase activity was detected 24 hr after transfection using the Dual-Luciferase Reporter Assay System (Promega, Beijing, China) as described previously.[32] Each experiment was repeated at least three times independently.

Exosome Isolation

H9c2 cells were transfected with miR-217 mimics for 24 hr, and then the culture media were collected and centrifuged at $2,000 \times g$ for 30 min at room temperature. The supernatants were transferred into new tubes, mixed with exosome isolation reagent, and stored at 4°C overnight. Then the mixtures were centrifuged at $1,500 \times g$ for 30 min at 4°C, and the supernatants were discarded following the manufacturer's instructions. The pellets were resuspended in PBS. To confirm that the RNA was confined in the exosomes, the exosomes were treated with 0.4 μg/μL RNase for 10 min at 37°C as described previously.[22]

Cell Viability

Fibroblasts were seeded in 96-well plates, and 24 hr later, they were transfected with cardiomyocyte-derived exosomes in 10 μL. Twenty-four hours later, 10 μL CCK8 reagent (Beyotime, Shanghai, China) was added per well, and the cells were cultured at 37°C for 0.5, 1, and 2 hr, respectively. The absorbance was detected at 450 nm following the manufacturer's recommendations.

Statistical Analysis

Data are presented as mean ± SEM. Comparisons between two groups were performed with Student's t tests. For comparisons of more than 2 groups, one-way ANOVA was used. Linear correlation was analyzed using Pearson correlation analysis. Values of p < 0.05 were considered statistically significant.

SUPPLEMENTAL INFORMATION

Supplemental Information includes three figures and nine tables and can be found with this article online at https://doi.org/10.1016/j.omtn.2018.05.013.

AUTHOR CONTRIBUTIONS

X.N. designed the study, analyzed and interpreted the data, and drafted the paper. J.F. and H.L. designed and analyzed the data. Z.Y., Y.Z., and B.D. participated in acquiring the data. N.D., C.C., and D.W.W. designed the work and drafted the paper.

CONFLICTS OF INTEREST

We declare no competing financial interests.

ACKNOWLEDGMENTS

REFERENCES

1. Frey, N., and Olson, E.N. (2003). Cardiac hypertrophy: the good, the bad, and the ugly. Annu. Rev. Physiol. 65, 45–79.

2. Heineke, J., Kempf, T., Kraft, T., Hilfiker, A., Morawietz, H., Scheubel, R.J., Caroni, P., Lohmann, S.M., Drexler, H., and Wollert, K.C. (2003). Downregulation of cytoskeletal muscle LIM protein by nitric oxide: impact on cardiac myocyte hypertrophy. Circulation 107, 1424–1432.

3. Petrov, G., Regitz-Zagrosek, V., Lehmkuhl, E., Krabatsch, T., Dunkel, A., Dandel, M., Dworatzek, E., Mahmoodzadeh, S., Schubert, C., Becher, E., et al. (2010). Regression of myocardial hypertrophy after aortic valve replacement: faster in women? Circulation 122 (11, Suppl), S23–S28.

4. Marques, F.Z., Nelson, E., Chu, P.Y., Horlock, D., Fiedler, A., Ziemann, M., Tan, J.K., Kuruppu, S., Rajapakse, N.W., El-Osta, A., et al. (2017). High-Fiber Diet and Acetate Supplementation Change the Gut Microbiota and Prevent the Development of Hypertension and Heart Failure in Hypertensive Mice. Circulation 135, 964–977.

5. Bernardo, B.C., Weeks, K.L., Pretorius, L., and McMullen, J.R. (2010). Molecular distinction between physiological and pathological cardiac hypertrophy: experimental findings and therapeutic strategies. Pharmacol. Ther. 128, 191–227.

6. Chow, S.L., Maisel, A.S., Anand, I., Bozkurt, B., de Boer, R.A., Felker, G.M., Fonarow, G.C., Greenberg, B., Januzzi, J.L., Jr., Kiernan, M.S., et al.; American Heart Association Clinical Pharmacology Committee of the Council on Clinical Cardiology; Council on Basic Cardiovascular Sciences; Council on Cardiovascular Disease in the Young; Council on Cardiovascular and Stroke Nursing; Council on Cardiopulmonary, Critical Care, Perioperative and Resuscitation; Council on Epidemiology and Prevention; Council on Functional Genomics and Translational Biology; and Council on Quality of Care and Outcomes Research (2017). Role of Biomarkers for the Prevention, Assessment, and Management of Heart Failure: A Scientific Statement From the American Heart Association. Circulation 135, e1054–e1091.

7. London, B. (2006). Natriuretic peptides and cardiac hypertrophy. J. Am. Coll. Cardiol. 48, 506–507.

8. Shende, P., Plaisance, I., Morandi, C., Pellieux, C., Berthonneche, C., Zorzato, F., Krishnan, J., Lerch, R., Hall, M.N., Rüegg, M.A., et al. (2011). Cardiac raptor ablation impairs adaptive hypertrophy, alters metabolic gene expression, and causes heart failure in mice. Circulation 123, 1073–1082.

9. Lai, E.C. (2002). Micro RNAs are complementary to 3′ UTR sequence motifs that mediate negative post-transcriptional regulation. Nat. Genet. 30, 363–364.

10. Bartel, D.P. (2004). MicroRNAs: genomics, biogenesis, mechanism, and function. Cell 116, 281–297.

11. Yan, M., Chen, C., Gong, W., Yin, Z., Zhou, L., Chaugai, S., and Wang, D.W. (2015). miR-21-3p regulates cardiac hypertrophic response by targeting histone deacetylase-8. Cardiovasc. Res. 105, 340–352.

12. Yang, Y., Del Re, D.P., Nakano, N., Sciarretta, S., Zhai, P., Park, J., Sayed, D., Shirakabe, A., Matsushima, S., Park, Y., et al. (2015). miR-206 Mediates YAP-Induced Cardiac Hypertrophy and Survival. Circ. Res. *117*, 891–904.

13. Callis, T.E., Pandya, K., Seok, H.Y., Tang, R.H., Tatsuguchi, M., Huang, Z.P., Chen, J.F., Deng, Z., Gunn, B., Shumate, J., et al. (2009). MicroRNA-208a is a regulator of cardiac hypertrophy and conduction in mice. J. Clin. Invest. *119*, 2772–2786.

14. Carè, A., Catalucci, D., Felicetti, F., Bonci, D., Addario, A., Gallo, P., Bang, M.L., Segnalini, P., Gu, Y., Dalton, N.D., et al. (2007). MicroRNA-133 controls cardiac hypertrophy. Nat. Med. *13*, 613–618.

15. Li, H., Fan, J., Yin, Z., Wang, F., Chen, C., and Wang, D.W. (2016). Identification of cardiac-related circulating microRNA profile in human chronic heart failure. Oncotarget *7*, 33–45.

16. van Rooij, E., Sutherland, L.B., Liu, N., Williams, A.H., McAnally, J., Gerard, R.D., Richardson, J.A., and Olson, E.N. (2006). A signature pattern of stress-responsive microRNAs that can evoke cardiac hypertrophy and heart failure. Proc. Natl. Acad. Sci. USA *103*, 18255–18260.

17. Thienpont, B., Aronsen, J.M., Robinson, E.L., Okkenhaug, H., Loche, E., Ferrini, A., Brien, P., Alkass, K., Tomasso, A., Agrawal, A., et al. (2017). The H3K9 dimethyl-transferases EHMT1/2 protect against pathological cardiac hypertrophy. J. Clin. Invest. *127*, 335–348.

18. Ibrahim, A., and Marbán, E. (2016). Exosomes: Fundamental Biology and Roles in Cardiovascular Physiology. Annu. Rev. Physiol. *78*, 67–83.

19. Mathiyalagan, P., and Sahoo, S. (2017). Exosomes-Based Gene Therapy for MicroRNA Delivery. Methods Mol. Biol. *1521*, 139–152.

20. Ong, S.G., Lee, W.H., Huang, M., Dey, D., Kodo, K., Sanchez-Freire, V., Gold, J.D., and Wu, J.C. (2014). Cross talk of combined gene and cell therapy in ischemic heart disease: role of exosomal microRNA transfer. Circulation *130* (11, Suppl 1), S60–S69.

21. Davidson, S.M., Takov, K., and Yellon, D.M. (2017). Exosomes and Cardiovascular Protection. Cardiovasc. Drugs Ther. *31*, 77–86.

22. Valadi, H., Ekström, K., Bossios, A., Sjöstrand, M., Lee, J.J., and Lötvall, J.O. (2007). Exosome-mediated transfer of mRNAs and microRNAs is a novel mechanism of genetic exchange between cells. Nat. Cell Biol. *9*, 654–659.

23. Barile, L., Moccetti, T., Marbán, E., and Vassalli, G. (2017). Roles of exosomes in cardioprotection. Eur. Heart J. *38*, 1372–1379.

24. Bang, C., Batkai, S., Dangwal, S., Gupta, S.K., Foinquinos, A., Holzmann, A., Just, A., Remke, J., Zimmer, K., Zeug, A., et al. (2014). Cardiac fibroblast-derived microRNA passenger strand-enriched exosomes mediate cardiomyocyte hypertrophy. J. Clin. Invest. *124*, 2136–2146.

25. Xiao, J., Pan, Y., Li, X.H., Yang, X.Y., Feng, Y.L., Tan, H.H., Jiang, L., Feng, J., and Yu, X.Y. (2016). Cardiac progenitor cell-derived exosomes prevent cardiomyocytes apoptosis through exosomal miR-21 by targeting PDCD4. Cell Death Dis. *7*, e2277.

26. Crackower, M.A., Oudit, G.Y., Kozieradzki, I., Sarao, R., Sun, H., Sasaki, T., Hirsch, E., Suzuki, A., Shioi, T., Irie-Sasaki, J., et al. (2002). Regulation of myocardial contractility and cell size by distinct PI3K-PTEN signaling pathways. Cell *110*, 737–749.

27. Kato, M., Putta, S., Wang, M., Yuan, H., Lanting, L., Nair, I., Gunn, A., Nakagawa, Y., Shimano, H., Todorov, I., et al. (2009). TGF-beta activates Akt kinase through a microRNA-dependent amplifying circuit targeting PTEN. Nat. Cell Biol. *11*, 881–889.

28. Shao, Y., Lv, C., Wu, C., Zhou, Y., and Wang, Q. (2016). Mir-217 promotes inflammation and fibrosis in high glucose cultured rat glomerular mesangial cells via Sirt1/HIF-1α signaling pathway. Diabetes Metab. Res. Rev. *32*, 534–543.

29. Han, F., Konkalmatt, P., Chen, J., Gildea, J., Felder, R.A., Jose, P.A., and Armando, I. (2015). MiR-217 mediates the protective effects of the dopamine D2 receptor on fibrosis in human renal proximal tubule cells. Hypertension *65*, 1118–1125.

30. Deng, S., Zhu, S., Wang, B., Li, X., Liu, Y., Qin, Q., Gong, Q., Niu, Y., Xiang, C., Chen, J., et al. (2014). Chronic pancreatitis and pancreatic cancer demonstrate active epithelial-mesenchymal transition profile, regulated by miR-217-SIRT1 pathway. Cancer Lett. *355*, 184–191.

31. Xie, J., Ameres, S.L., Friedline, R., Hung, J.H., Zhang, Y., Xie, Q., Zhong, L., Su, Q., He, R., Li, M., et al. (2012). Long-term, efficient inhibition of microRNA function in mice using rAAV vectors. Nat. Methods *9*, 403–409.

32. Fan, J., Li, H., Nie, X., Yin, Z., Zhao, Y., Chen, C., and Wen Wang, D. (2017). MiR-30c-5p ameliorates hepatic steatosis in leptin receptor-deficient (db/db) mice via down-regulating FASN. Oncotarget *8*, 13450–13463.

33. Worby, C.A., and Dixon, J.E. (2014). Pten. Annu. Rev. Biochem. *83*, 641–669.

34. Oudit, G.Y., and Penninger, J.M. (2009). Cardiac regulation by phosphoinositide 3-kinases and PTEN. Cardiovasc. Res. *82*, 250–260.

35. Oudit, G.Y., Sun, H., Kerfant, B.G., Crackower, M.A., Penninger, J.M., and Backx, P.H. (2004). The role of phosphoinositide-3 kinase and PTEN in cardiovascular physiology and disease. J. Mol. Cell. Cardiol. *37*, 449–471.

36. Shioi, T., Kang, P.M., Douglas, P.S., Hampe, J., Yballe, C.M., Lawitts, J., Cantley, L.C., and Izumo, S. (2000). The conserved phosphoinositide 3-kinase pathway determines heart size in mice. EMBO J. *19*, 2537–2548.

37. Guillermet-Guibert, J., Bjorklof, K., Salpekar, A., Gonella, C., Ramadani, F., Bilancio, A., Meek, S., Smith, A.J., Okkenhaug, K., and Vanhaesebroeck, B. (2008). The p110beta isoform of phosphoinositide 3-kinase signals downstream of G protein-coupled receptors and is functionally redundant with p110gamma. Proc. Natl. Acad. Sci. USA *105*, 8292–8297.

38. Xu, X.D., Song, X.W., Li, Q., Wang, G.K., Jing, Q., and Qin, Y.W. (2012). Attenuation of microRNA-22 derepressed PTEN to effectively protect rat cardiomyocytes from hypertrophy. J. Cell. Physiol. *227*, 1391–1398.

39. Jonas, S., and Izaurralde, E. (2015). Towards a molecular understanding of microRNA-mediated gene silencing. Nat. Rev. Genet. *16*, 421–433.

40. Ren, X.P., Wu, J., Wang, X., Sartor, M.A., Jones, K., Qian, J., Nicolaou, P., Pritchard, T.J., and Fan, G.C. (2009). MicroRNA-320 is involved in the regulation of cardiac ischemia/reperfusion injury by targeting heat-shock protein 20. Circulation *119*, 2357–2366.

41. Wahlquist, C., Jeong, D., Rojas-Muñoz, A., Kho, C., Lee, A., Mitsuyama, S., van Mil, A., Park, W.J., Sluijter, J.P., Doevendans, P.A., et al. (2014). Inhibition of miR-25 improves cardiac contractility in the failing heart. Nature *508*, 531–535.

42. Manabe, I., Shindo, T., and Nagai, R. (2002). Gene expression in fibroblasts and fibrosis: involvement in cardiac hypertrophy. Circ. Res. *91*, 1103–1113.

43. Bauersachs, J. (2010). Regulation of myocardial fibrosis by MicroRNAs. J. Cardiovasc. Pharmacol. *56*, 454–459.

44. Zhao, Q.D., Viswanadhapalli, S., Williams, P., Shi, Q., Tan, C., Yi, X., Bhandari, B., and Abboud, H.E. (2015). NADPH oxidase 4 induces cardiac fibrosis and hypertrophy through activating Akt/mTOR and NFκB signaling pathways. Circulation *131*, 643–655.

45. Chen, S., Puthanveetil, P., Feng, B., Matkovich, S.J., Dorn, G.W., 2nd, and Chakrabarti, S. (2014). Cardiac miR-133a overexpression prevents early cardiac fibrosis in diabetes. J. Cell. Mol. Med. *18*, 415–421.

46. Matkovich, S.J., Wang, W., Tu, Y., Eschenbacher, W.H., Dorn, L.E., Condorelli, G., Diwan, A., Nerbonne, J.M., and Dorn, G.W., 2nd (2010). MicroRNA-133a protects against myocardial fibrosis and modulates electrical repolarization without affecting hypertrophy in pressure-overloaded adult hearts. Circ. Res. *106*, 166–175.

47. Lyu, L., Wang, H., Li, B., Qin, Q., Qi, L., Nagarkatti, M., Nagarkatti, P., Janicki, J.S., Wang, X.L., and Cui, T. (2015). A critical role of cardiac fibroblast-derived exosomes in activating renin angiotensin system in cardiomyocytes. J. Mol. Cell. Cardiol. *89* (Pt B), 268–279.

48. Wang, C., Zhang, C., Liu, L., A X, Chen, B., Li, Y., and Du, J. (2017). Macrophage-Derived mir-155-Containing Exosomes Suppress Fibroblast Proliferation and Promote Fibroblast Inflammation during Cardiac Injury. Mol. Ther *25*, 192–204.

49. Wang, J., Huang, W., Thibault, S., Brown, T.P., Bobrowski, W., Gukasyan, H.J., Evering, W., Hu, W., John-Baptiste, A., and Vitsky, A. (2017). Evaluation of miR-216a and miR-217 as Potential Biomarkers of Acute Exocrine Pancreatic Toxicity in Rats. Toxicol. Pathol. *45*, 321–334.

50. Hergenreider, E., Heydt, S., Tréguer, K., Boettger, T., Horrevoets, A.J.G., Zeiher, A.M., Scheffer, M.P., Frangakis, A.S., Yin, X., Mayr, M., et al. (2012). Atheroprotective communication between endothelial cells and smooth muscle cells through miRNAs. Nat. Cell Biol. *14*, 249–256.

51. Pironti, G., Strachan, R.T., Abraham, D., Mon-Wei Yu, S., Chen, M., Chen, W., Hanada, K., Mao, L., Watson, L.J., and Rockman, H.A. (2015). Circulating

Exosomes Induced by Cardiac Pressure Overload Contain Functional Angiotensin II Type 1 Receptors. Circulation *131*, 2120–2130.

52. Beltrami, C., Besnier, M., Shantikumar, S., Shearn, A.I.U., Rajakaruna, C., Laftah, A., Sessa, F., Spinetti, G., Petretto, E., Angelini, G.D., and Emanueli, C. (2017). Human Pericardial Fluid Contains Exosomes Enriched with Cardiovascular-Expressed MicroRNAs and Promotes Therapeutic Angiogenesis. Mol. Ther. *25*, 679–693.

53. Li, H., Zhang, X., Wang, F., Zhou, L., Yin, Z., Fan, J., Nie, X., Wang, P., Fu, X.D., Chen, C., and Wang, D.W. (2016). MicroRNA-21 Lowers Blood Pressure in Spontaneous Hypertensive Rats by Upregulating Mitochondrial Translation. Circulation *134*, 734–751.

54. Cingolani, O.H., Yang, X.P., Cavasin, M.A., and Carretero, O.A. (2003). Increased systolic performance with diastolic dysfunction in adult spontaneously hypertensive rats. Hypertension *41*, 249–254.